

Rotational isomerism and crystal structures of 9,9'-dicyano-9,9'-bifluorenyl and 9,9'-dinitro-9,9'-bifluorenyl



Yu-Lin Lam,* Lip-Lin Koh, Hsing-Hua Huang and Li Wang

Department of Chemistry, National University of Singapore, Lower Kent Ridge Road, Singapore 119260. E-mail: chmlamyl@nus.edu.sg

Received (in Cambridge) 4th February 1999, Accepted 25th March 1999

Dipole moments of the compounds 9,9'-dicyano-9,9'-bifluorenyl **1** and 9,9'-dinitro-9,9'-bifluorenyl **2** in 1,4-dioxane and benzene have been measured over a range of temperatures. The crystal and molecular structures of the compounds were determined by single-crystal X-ray diffraction methods. Analyses of the crystal structures and relative permittivity data show that the compounds exist in the polar *gauche* conformation in the solid state and as rotameric mixtures in solution with a predominantly high *gauche* population of 94% and 99% respectively at 25 °C. The experimentally derived values of the energy difference between the *gauche* and *trans* rotamers and the *gauche/trans* population quotients were compared with the values predicted by the semiempirical MO programme AMPAC using AM1 parametrization. Dynamic ¹H NMR was employed to determine the activation parameters for the barriers to rotation in solution.

Introduction

Our interest in polar and steric effects on rotational isomerism in symmetrically substituted ethanes has led us to investigate the influence of the cyano and nitro groups in such molecules. Earlier works on 1,2-dicyanoethane¹ and 1,2-dinitroethane² have shown that these compounds prefer the *gauche* conformation. However studies on dicyano and dinitro compounds containing phenyl and alkyl substituents have shown contrasting results with the dicyano series of compounds existing mainly in the *trans* form and the dinitro compounds favouring the *gauche* conformation.^{3–7} We now report our findings on the back-clamped molecules, 9,9'-dicyano-9,9'-bifluorenyl **1** and 9,9'-dinitro-9,9'-bifluorenyl **2**, based on dipole moment determination, X-ray diffraction measurements and ¹H NMR spectroscopy. We have also compared observed energy differences between *gauche* and *trans* rotamers and *gauche/trans* population ratios with predictions made by semiempirical molecular orbital calculations.

Experimental

Preparation of compounds

Compound **1** was synthesised in three steps from fluorene by a procedure based on the methods of Matthews,⁸ Wislicenus⁹ and Kharasch.¹⁰ It had mp 264.5–265.5 °C (decomp.) (from glacial acetic acid) (lit.,¹¹ 265–268 °C) (Found: C, 88.46; H, 4.26; N, 7.26. C₂₈H₁₆N₂ requires C, 88.40; H, 4.24; N, 7.36%). Compound **2** was prepared by the method of Wislicenus¹² and Pagano.¹³ It had mp 180–181 °C (decomp.) (lit.,¹³ 181–182 °C) (Found: C, 74.55; H, 3.96; N, 6.17. C₂₆H₁₆N₂O₄ requires C, 74.30; H, 3.81; N, 6.66%).

Dipole moment determination

Relative permittivities were determined with a heterodyne-beat meter¹⁴ and densities and refractive indices by standard procedures.¹⁵ Benzene was carefully distilled and stored over sodium before use. 1,4-Dioxane, when used as a solvent, was freshly distilled after continuous reflux over sodium. The physical constants required in the permittivity measurements have been given previously.^{6,16}

Calculations

Semiempirical molecular orbital calculations were performed using the programme¹⁷ AMPAC 5.0 with AM1 parametrization.¹⁸ Structural parameters used were taken from our X-ray diffraction results of the compounds. Full geometry optimization was performed for each incremental value of the ethane C–C torsion angle which was defined by the atoms CN–C–CN for **1** and N–C–C–N for **2** by the convention of Klyne and Prelog.¹⁹

Crystal structure determination and refinement †

Single crystals of **1** were obtained from glacial acetic acid and **2** from benzene–light petroleum (40–70 °C). Crystallisation of **2** proved extremely difficult because the crystals were often soft and poorly formed. As a consequence the extent of the data obtained was limited and the precision of the structure reduced.

Crystal data of **1**: C₂₈H₁₆N₂, *M* = 380.4. Monoclinic, colourless prisms, *a* = 14.810(3), *b* = 16.056(3), *c* = 18.079(4) Å, β = 110.97(3)°, *V* = 4014(2) Å³, space group *P*2₁/*c*, *Z* = 8, *D*_x = 1.259 g cm⁻³. Crystal dimension: 0.40 × 0.40 × 0.25, μ(Mo-Kα) = 0.074 mm⁻¹. Crystal data of **2**: C₂₆H₁₆N₂O₄, *M* = 420.4. Monoclinic, colourless blocks, *a* = 8.990(2), *b* = 16.499(7), *c* = 13.445(3) Å, β = 94.78(2)°, *V* = 1987.4(9) Å³, space group *P*2₁/*n*, *Z* = 4, *D*_x = 1.405 g cm⁻³. Crystal dimension: 0.40 × 0.35 × 0.28, μ(Mo-Kα) = 0.096 mm⁻¹.

Data collections were performed at room temperature using a Siemens R3m/V200 diffractometer with Mo-Kα radiation (λ = 0.71060 Å). For **1**, a total of 7098 independent reflections were recorded with 3.5 < 2θ < 50.0° of which 3591 with *I* > 2σ(*I*) were considered unique and observed. In **2**, a total of 3749 independent reflections were measured (3.5 < 2θ < 50.0°) of which 3513 had *I* > 2σ(*I*). Cell constants for both compounds were determined by least-squares fit to the setting parameters of 15 reflections. Intensity data were collected by Wyckoff scan. Linear and approximate isotropic crystal decay, ca. 25% was corrected during processing of crystals **1** and **2**.

Lorentz and polarization corrections, structure solution by direct methods, full-matrix least-squares refinements and

† CCDC reference number 188/163.

Table 1 Molar polarization, refractions and dipole moments at infinite dilution of 9-cyanofluorene, 9,9'-dicyano-9,9'-bifluorenyl **1** and 9,9'-dinitro-9,9'-bifluorenyl **2**

<i>T</i> /°C	Solvent	Conc. range/10 ⁵ <i>w</i> ₂	<i>aε</i> ₁	<i>β</i>	<i>γ</i>	<i>P</i> ₂ /cm ³	<i>R</i> _D /cm ³	<i>μ</i> ^a /10 ³⁰ C m
9-Cyanofluorene (<i>R</i> _D = 57.34 cal)								
25	1,4-dioxane	240–600	6.19	0.262	0.080	235.1	57.35	9.75 ± 0.03
45	1,4-dioxane	240–600	6.15	0.441		231.4		9.95 ± 0.02
60	1,4-dioxane	240–600	6.12	0.609		225.5		10.03 ± 0.04
9,9'-Dicyano-9,9'-bifluorenyl 1 (<i>R</i> _D = 112.63 cal)								
25	1,4-dioxane	420–730	7.99	0.261	0.080	580.4	114.33	15.84 ± 0.04
45	1,4-dioxane	420–730	7.33	0.346		546.9		15.76 ± 0.07
60	1,4-dioxane	420–730	6.86	0.384		514.4		15.50 ± 0.04
9,9'-Dinitro-9,9'-bifluorenyl 2 (<i>R</i> _D = 115.10 cal)								
25	Benzene	135–230	8.10	0.667	0.366	703.5	113.04	17.85 ± 0.02
45	Benzene	135–230	7.66	0.855		652.5		17.61 ± 0.02
60	Benzene	135–230	7.10	0.869		624.5		17.54 ± 0.01

^a *P*_D = 1.05*R*_D.

Table 2 Bond lengths (Å), bond angles and torsion angles (°) of **1**

C(9)–C(10)	1.534(3)	C(9)–C(13)	1.534(4)
C(9)–C(14)	1.477(4)	C(9)–C(9')	1.612(4)
C(11)–C(12)	1.461(4)	C(14)–N(14)	1.143(4)
C(29)–C(30)	1.528(3)	C(29)–C(33)	1.529(4)
C(29)–C(34)	1.481(4)	C(29)–C(29')	1.611(4)
C(34')–N(34')	1.142(4)	C(31)–C(32)	1.460(4)
C(10)–C(9)–C(13)	101.7(2)	C(10)–C(9)–C(14)	110.0(2)
C(13)–C(9)–C(14)	111.4(3)	C(10)–C(9)–C(9')	112.0(2)
C(13)–C(9)–C(9')	110.6(2)	C(14)–C(9)–C(9')	109.8(2)
C(4)–C(11)–C(12)	130.6(3)	C(5)–C(12)–C(11)	130.9(3)
C(9)–C(13)–C(12)	109.6(2)	C(1')–C(10')–C(9')	129.2(2)
C(30)–C(29)–C(33)	102.1(2)	C(30)–C(29)–C(34)	110.7(2)
C(33)–C(29)–C(34)	112.2(2)	C(30)–C(29)–C(29')	112.3(2)
C(33)–C(29)–C(29')	110.6(2)	C(34)–C(29)–C(29')	108.8(2)
C(29)–C(30)–C(31)	109.8(2)	C(24)–C(31)–C(32)	131.4(3)
C(25)–C(32)–C(31)	130.4(2)	C(29)–C(33)–C(32)	109.1(2)
C(2)–C(1)–C(10)–C(9)	175.5(3)	C(3)–C(4)–C(11)–C(12)	–179.9(3)
C(10)–C(9)–C(9')–C(10')	–169.1(2)	C(14)–C(9)–C(9')–C(14')	–55.4(3)
C(30)–C(29)–C(29')–C(30')	–172.3(2)	C(34)–C(29)–C(29')–C(34')	–57.9(3)
C(6)–C(5)–C(12)–C(11)	–175.9(3)	C(24)–C(31)–C(32)–C(25)	–3.5(6)
C(24')–C(31')–C(32')–C(25')	–1.3(7)		

preparation of figures were all performed by the programs of SHELXTL-Plus.²⁰ All non-hydrogen atoms were refined anisotropically whereas hydrogen atoms were placed at calculated positions with the isotropic displacement coefficient being assigned a value that is 1.6 times that of the atom to which it is attached. The weighting scheme $w = 1/[\sigma^2(F_o) + 0.0040F_o^2]$ gave satisfactory agreement analyses. For **1**, the final *R* and *R*_w factors obtained after refinement of 542 parameters were 4.03 and 5.57% respectively whilst in **2**, the values obtained after refinement of 290 parameters were 8.99 and 7.76%. The largest peaks in the final Fourier difference maps of **1** and **2** are 0.15 and 0.60 e Å^{–3} respectively.

Dynamic NMR measurements

All NMR spectra were recorded on a Bruker AMX-500 FTNMR spectrometer equipped with a variable temperature probe. CD₂Cl₂ was used as a solvent and tetramethylsilane as an internal standard.

Results and discussion

The results of the dipole moment measurements of **1** and **2** are presented in Table 1 with standard notation. Three concentration dependencies, namely those of the relative permittivities, densities and refractive indices (*aε*₁, *βd*₁ and *γd*₁₂) were

determined for each solvent at the three temperatures. Using the least squares method, the experimental values of the slope *aε*₁, *βd*₁ and *γm*₁², given by eqns. (1)–(3), at infinite dilutions of

$$a\varepsilon_1 = \left(\frac{\delta\Delta\varepsilon}{\delta w_2} \right)_{w_2 \rightarrow 0} \quad (1)$$

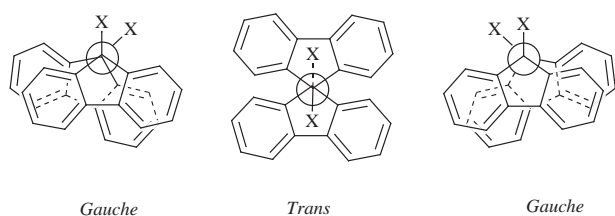
$$\beta d_1 = \left(\frac{\delta\Delta d}{\delta w_2} \right)_{w_2 \rightarrow 0} \quad (2)$$

$$\gamma m_1^2 = \left(\frac{\delta\Delta n^2}{\delta w_2} \right)_{w_2 \rightarrow 0} \quad (3)$$

the compounds (*w*₂ denoting the solute weight fraction) and the respective molar polarization, refractions and dipole moments were calculated. The dipole moments were determined using the method of LeFevre and Vines.²¹ Dipole moments of **1** were determined in 1,4-dioxane as it was virtually insoluble in common non-polar solvents. The dipole moment of 9-cyanofluorene, being needed in the calculation for the dipole moment of the different conformations of **1**, has also been measured in 1,4-dioxane at the various temperatures and the results are included in Table 1. Bond lengths, bond angles and torsion angles of **1** and **2** are given in Tables 2 and 3. Fig. 1 shows the stable conformations of both the compounds where the two

Table 3 Bond lengths (Å), bond angles and torsion angles (°) of **2**

C(9)–C(10)	1.521(4)	C(9)–C(13)	1.525(4)
C(9)–C(9')	1.584(4)	C(9)–N(1)	1.545(4)
C(11)–C(12)	1.454(4)	N(1)–O(12)	1.178(5)
N(1)–O(11)	1.200(4)	N(1')–O(12')	1.199(6)
N(1')–O(11')	1.158(5)		
C(10)–C(9)–C(13)	103.0(2)	C(10)–C(9)–C(9')	114.2(2)
C(13)–C(9)–C(9')	109.3(2)	C(10)–C(9)–N(1)	109.5(2)
C(13)–C(9)–N(1)	110.1(2)	C(9')–C(9)–N(1)	110.5(2)
C(1)–C(10)–C(9)	131.0(3)	O(11)–N(1)–O(12)	122.4(3)
O(11')–N(1')–O(12')	123.4(3)		
C(2)–C(1)–C(10)–C(9)	178.5(3)	C(3)–C(4)–C(11)–C(12)	177.4(3)
C(6)–C(5)–C(12)–C(11)	–176.9(3)	C(7)–C(8)–C(13)–C(9)	–177.4(3)
C(13)–C(9)–C(10)–C(1)	174.6(3)	C(13)–C(9)–C(10)–C(11)	–5.7(3)
C(9')–C(9)–C(10)–C(1)	–67.0(4)	N(1)–C(9)–C(10)–C(1)	57.5(4)
C(9')–C(9)–C(13)–C(8)	–63.7(3)	N(1)–C(9)–C(13)–C(8)	–57.9(3)
C(10)–C(9)–C(9')–C(10')	–178.0(2)	N(1)–C(9)–C(9')–C(10')	58.1(3)
C(9)–C(10)–C(11)–C(12)	3.3(3)	C(4)–C(11)–C(12)–C(13)	–176.8(3)

**Fig. 1** Stable conformations of 9,9'-disubstituted-9,9'-bifluorenyl (X = CN, NO₂).

gauche rotamers are mirror images of each other and are in dynamic equilibrium with the *trans* rotamer in solution.

Dipole moment measurements of **1**

The large dipole moment means that the polar *gauche* rotamers must be present in high proportion in this solvent. From Table 1, it can also be seen that the dipole moment of the compound decreases with increasing temperature in 1,4-dioxane, indicating that the *gauche* rotamer is more stable than the *trans*, and is higher in population in this solvent.

The resultant dipole moment $\mu(2\theta)$ of any rotamer of a molecule YCR₂–CR₂Y may be expressed using eqn. (4), where μ_o is

$$\mu_g = \mu(2\theta) = 2\mu_o \sin a \cos \theta \quad (4)$$

the moment of the symmetrical half of the molecule (CR₂Y), a is the supplement of the central C–C–Y bond angle and 2θ is the dihedral angle between the two C–C–Y planes.²² In our calculations on **1**, μ_o was taken to be the value of the dipole moment of 9-cyanofluorene with its direction along the C–CN bond while the values of a (71.18°) and 2θ (55.4°) were taken from the results of our X-ray diffraction study of the molecule. Substitution of these values into eqn. (4) gives a dipole moment (μ_g) of 16.34×10^{-30} C m for the *gauche* rotamer.

Assuming that μ_g is independent of temperature, an estimate of the *gauche* rotamer population ($x\%$) in solution can be made from eqn. (5), which on substituting the observed moment and μ_g values yields a population of 94% *gauche* and 6% *trans* at 25 °C.

$$x = \frac{100\mu_{\text{obs}}^2}{\mu_g^2} \quad (5)$$

The very high proportion of the *gauche* rotamer suggests that in this compound, the *gauche* conformation is inherently much more stable than the *trans*. According to Boltzmann's equation, the internal energy difference between the rotational isomers, $\Delta E = E_g - E_t$, of the molecule was calculated to be -5.10 kJ mol⁻¹.

These results contrast with 1,2-dicyanotetraphenylethane²³ which exists almost entirely in the *trans*-configuration with a ΔE value of 13.39–14.23 kJ mol⁻¹. This difference in conformational behaviour appears to be a manifestation of the effects of phenyl ring stacking in unclamped cyano-substituted polyarylethanes; it is consistent with the theory that there is a tendency for neighbouring phenyl rings in an unclamped polyarylethane to nest or stack so as to diminish the geminal repulsions and the valence angle spread.²⁴ This phenomenon is disallowed in back clamped molecules like **1** and thus the reversal of conformer preference could be attributed to the relief of the non-bonded steric interactions between the 1,8- and 1',8'-hydrogens in the *gauche* conformation. In the *trans* conformation the hydrogens on the 1,8-position of one fluorenyl moiety are forced to point directly at the hydrogens in the 1',8'-positions of the other fluorenyl ring, thus causing severe H···H non-bonded interactions.

Comparison of the decomposition temperatures of **1** and 1,2-dicyanotetraphenylethane²⁵ also clearly shows that the unclamped tetraphenylethane undergoes homolysis with greater ease. The stabilizing effect in **1** could be ascribed to the effects of back clamping that brings about a diminution in back strain, which arises from the non-bonded interactions between phenyl rings attached to the same ethane carbon, and front strain, which involves phenyl rings attached to different ethane carbons. Earlier studies²⁶ have shown the ability of back clamping to pin rings back, away from the region over the central bond, hence reducing front strain.

The variation of the heat of formation with the dihedral angle (2θ) obtained from AMPAC calculations with AM1 parametrization and full geometry optimization is shown in Fig. 2. Clearly, the *gauche* rotamer has a lower energy than the *trans* form, differing from it by 13.93 kJ mol⁻¹. The torsion angle of the *gauche* rotamer with the lowest energy was found to be 54° and the Boltzmann distribution to be 99.8% *gauche* and 0.2% *trans*. The difference of some 8.7 kJ mol⁻¹ between the calculated and experimentally derived energy difference is not entirely unexpected as (i) the AMPAC value represents the situation *in vacuo* which is likely to be modified in solution, and (ii) the effects of mutual induction of the cyano groups could possibly result in an overall lowering of the moment, thus causing the actual value of μ_o in eqn. (4) to be lower than the moment of 9-cyanofluorene.

X-Ray structure determination of 9,9'-dicyano-9,9'-bifluorenyl **1**

Each asymmetric unit of the cell contains two independent molecules in general positions. The inherent two-fold symmetry of the molecule is not utilized in the packing. Although the molecule does not have crystallographic symmetry, it shows

approximate two-fold rotational symmetry. Fig. 3 depicts the structure and defines the atomic numbering of the molecules. The independent molecules are essentially identical structures. Equivalent bond lengths and bond angles differed by less than 0.01 Å and 1° respectively.

Projection down the C(9)–C(9') bond clearly shows that **1** exists in the *gauche* conformation with the C(14)–C(9)–C(9')–C(14') and C(34)–C(29)–C(29')–C(34') torsion angles being –55.4 and –57.9° respectively. The same conformation has been observed in 9,9'-bifluorenyl,²⁷ 9*H*,9'*H*-hexadecachloro-9,9'-bifluorenyl²⁸ and has been predicted for other symmetrically aryl-substituted compounds containing two fluorenyl moieties.²⁷ Bond lengths and angles of **1** compare well with the corresponding ones of 9,9'-bifluorenyl, except for those involving the central atoms C(9) and C(9'). In the X-ray studies of

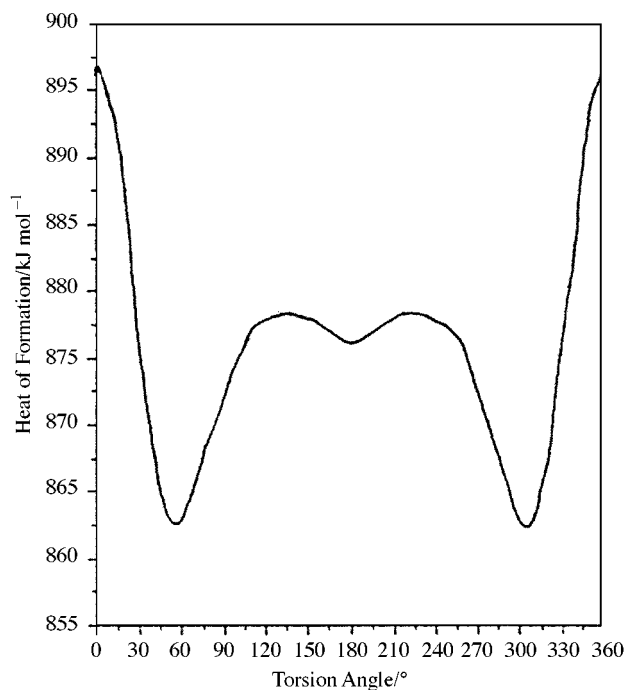


Fig. 2 Energy as a function of the CN–C–C–CN torsion angle as calculated by AMPAC.

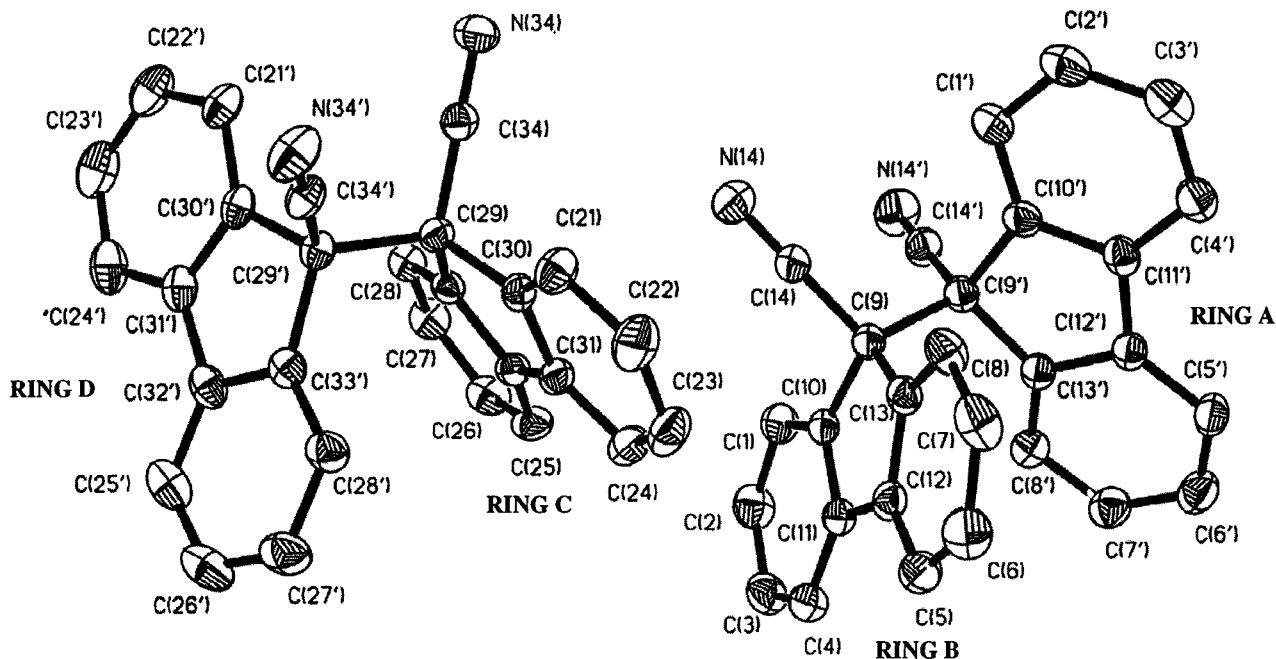


Fig. 3 Thermal ellipsoid diagram of **1**.

9,9'-bifluorenyl,²⁷ the central C–C bond length was found to be 1.542(3) Å, a value not significantly larger than that quoted for a standard tetrahedral C–C bond. By contrast, a value as large as 1.612(4) Å is observed for this distance in **1**, where a lengthening of the C(sp³)–C(sp²) bonds is also found [mean 1.532(3) Å vs. 1.515(3) Å in 9,9'-bifluorenyl and 1.468 Å in fluorene²⁹]. Values of the bond angles involving the two central atoms are listed in Table 2. The degree of deformation of the molecule is well documented by the marked deviations of some bond angles from the standard tetrahedral value. Of particular relevance are the closure of the C(10)–C(9)–C(12) bond angle to 101.7(2)° and the expansion of C(29)–C(29')–C(30') to 112.7(2)°. Evidently these deformations help to relieve the strong interactions between the fluorenyl moieties and the cyano groups, which are connected to the ethane framework by relatively long C(sp³)–C(sp) bonds of mean value 1.478(4) Å. The lengthening of the C(sp³)–C(sp) bond is not unexpected as similar bond lengths have been observed in other crowded molecules such as the 1,1'-dicyanobi(cycloalkane)s [*n* = 5–8, 1.475(6)–1.483(3) Å],^{30,31} 2,3-dicyano-2,3-diphenylbutane [1.481(3) Å] and 3,4-dicyano-3,4-diphenylhexane [1.477(3) Å].⁵

Further evidence for the steric hindrance in **1** is shown by the out-of-plane displacement of 0.08–0.14 Å in atoms C(9) and C(29) and the loss of planarity of the benzene groups in each fluorenyl system. The most significant deviation from planarity is observed in fluorenyl ring C in Fig. 3, where the largest displacement from the mean plane, 0.1337 Å, is observed for atom C(22). The two fluorenyl systems within each molecule are placed at 40.6° to each other.

Dipole moment measurement of **2**

Measurements were determined in benzene as **2** had very low solubility in carbon tetrachloride. The dipole moments of the compound in benzene ($\epsilon_{25} = 2.284$) are much higher than those of **1** in 1,4-dioxane ($\epsilon_{25} = 2.209$). Since the polarities of the cyano and nitro groups are virtually the same, this implies that the percentage of *gauche* rotamer in **2** is much higher than in **1**. Application of the Lennard–Jones–Pike³² method of analysis to our dipole moment data yields a ΔE value of $-9.67 \text{ kJ mol}^{-1}$ and a *gauche* conformer dipole moment (μ_g) of $17.92 \times 10^{-30} \text{ C m}$. From eqn. (5), the percentage *gauche* population at 25 °C was found to be 99%.

These values compare well with the results obtained from

AM1 calculations. The energy difference between the most stable calculated *gauche* form which has a dihedral angle of 54° and the *trans* rotamer, ΔE , is $-21.59 \text{ kJ mol}^{-1}$. From the Boltzmann equation, this would mean that **2** exists exclusively in the *gauche* form at 25°C .

X-Ray structure determination of 9,9'-dinitro-9,9'-bifluorenyl **2**

Molecules of **2** lie at general sites but, like in compound **1**, show approximate two-fold symmetry. Bond lengths, bond angles and torsion angles based on the final atomic positions are shown in Table 3.

The molecule as a whole adopts a *gauche* conformation with a $\text{N}(1)\text{-C}(9)\text{-C}(9')\text{-N}(1')$ torsion angle of $-65.5(3)^\circ$. The resulting structure (Fig. 4) shows that the two NO_2 groups are

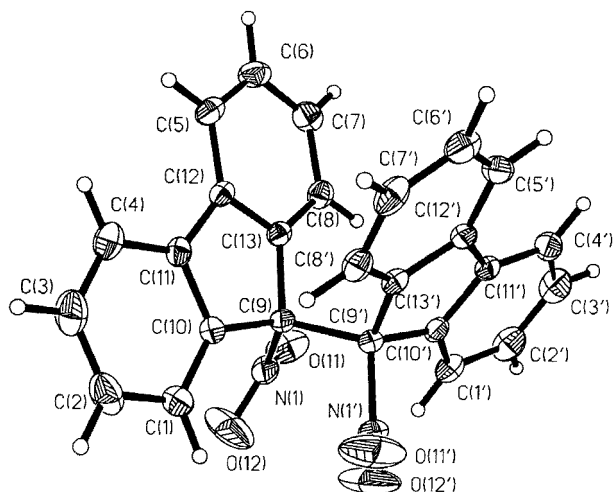


Fig. 4 Thermal ellipsoid diagram of **2**.

planar. An interesting feature of this molecule is that unlike other unclamped phenyl-substituted dinitroethanes⁴ and 1,2-dinitroethane,² both the NO_2 groups in structure **2** adopt a nearly perpendicular conformation with respect to the central C–C bond, the torsion angles $\text{C}(9')\text{-C}(9)\text{-N}(1)\text{-O}(12)$ and $\text{C}(9)\text{-C}(9')\text{-N}(1')\text{-O}(12')$ being $95.6(4)$ and $72.3(3)^\circ$ respectively. In this orientation, the O(12) and O(12') atoms are 2.829 \AA apart (*i.e.* the distance between the eclipsed oxygen atoms). Our earlier studies on various carbocyclic substituted dinitroethanes³³ have shown that as the ring size increases, the increasing ring strain would cause the NO_2 groups to rotate from a bisected conformation to a perpendicular conformation. In **2**, the fluorenyl moiety, with its clamped nature, may be viewed as a thirteen-membered carbocyclic ring and we may confidently ascribe the orientation of the NO_2 groups to the steric congestion in the fluorenyl rings. Comparison of the C–C(9)–C(9') or the C–C(9')–C(9) angles shows that those angles involving the sp^2 carbon which are synclinal to the opposite NO_2 group are significantly larger: $\text{C}(10)\text{-C}(9)\text{-C}(9')$ is $114.2(2)^\circ$ while $\text{C}(13)\text{-C}(9)\text{-C}(9')$ is $109.3(2)^\circ$, and $\text{C}(10')\text{-C}(9')\text{-C}(9)$ is $115.5(2)^\circ$ while $\text{C}(13')\text{-C}(9')\text{-C}(9)$ is $109.3(2)^\circ$. This observed widening is once again consistent with the existence of steric congestion in the molecule.

Least-squares analysis shows that the five-carbon-atom groups in the fluorenyl rings have envelope forms with atoms C(9) and C(9') deviating by 0.1 \AA from the tetraatomic plane. The fluorenyl groups within each molecule are placed at 50.0° to each other.

Dynamic NMR measurements of **1** and **2**

Fig. 5 shows the ^1H NMR spectra of **1** and **2** in dichloromethane- d_2 . At room temperature, both compounds exhibit spectra which are characteristic of first-order four-spin systems. However as the temperature decreases, the signals broaden,

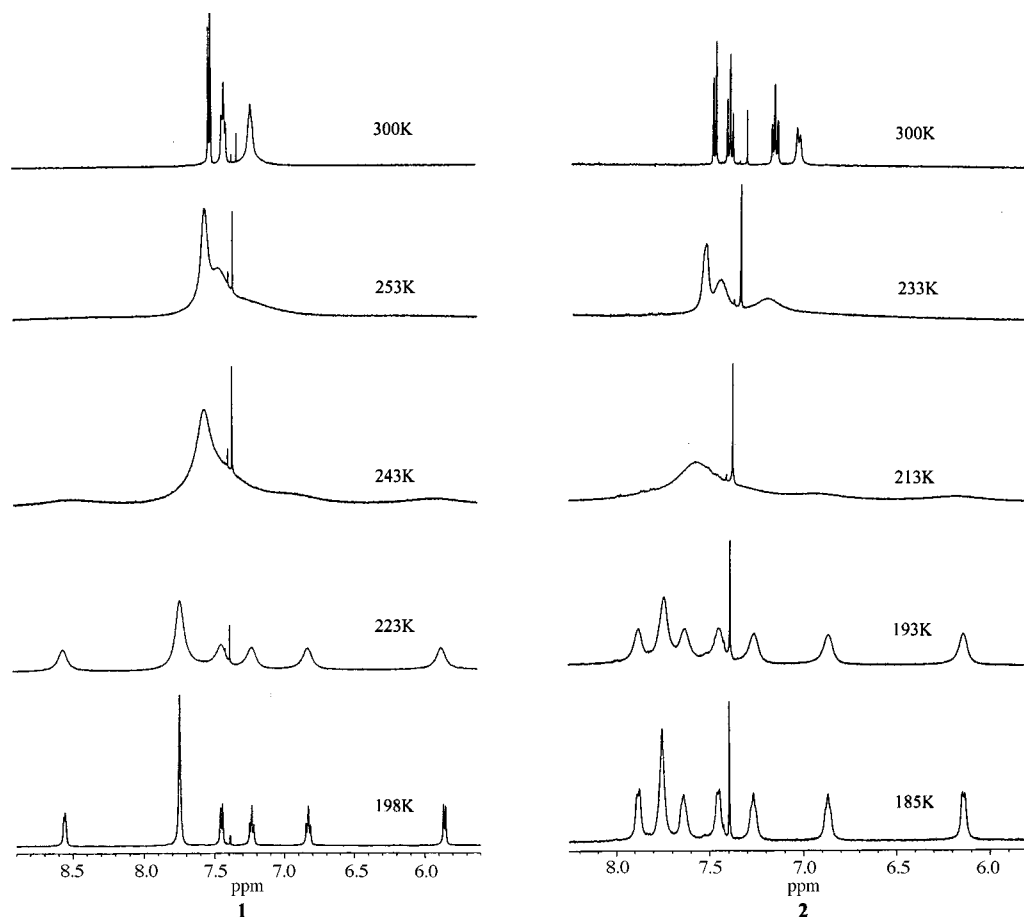


Fig. 5 Observed proton NMR spectra (500 MHz) of **1** and **2**.

Table 4 Activation parameters for the inversion of 9,9'-disubstituted-9,9'-bifluorenyls^a

Compound	T/K	$\Delta H^\ddagger/\text{kcal mol}^{-1}$	$\Delta S^\ddagger/\text{cal mol}^{-1} \text{K}^{-1}$	$\Delta G_{240}^\ddagger/\text{kcal mol}^{-1}$
9,9'-Bifluorenyl ^b	184–324	7.5	–10.8	9.9
9,9'-Dimethyl-9,9'-bifluorenyl ^b	195–324	6.3	–15.3	10.0
9,9'-Dichloro-9,9'-bifluorenyl ^b	257–348	12.2	–4.8	13.2
9,9'-Dibromo-9,9'-bifluorenyl ^b	257–348	12.2	–5.0	13.2
9,9'-Dicyano-9,9'-bifluorenyl	198–300	9.4	–7.5	11.2
9,9'-Dinitro-9,9'-bifluorenyl	185–300	8.6	–10.8	11.2

^a 1 cal = 4.1868 J. ^b Ref. 34.

coalesce to a broad singlet and then sharpen again to a well-resolved spectrum with the aromatic protons ranging from 8.57–5.85 ppm. The spectra of several other 9,9'-disubstituted-9,9'-bifluorenyls³⁴ have also shown analogous dynamic behaviour and the low temperature spectra were attributed to the two independent subspectra from the *gauche* conformation of the compounds. In this conformation, one of the phenyl rings in each fluorenyl fragment is placed within the shielding region of its companion fluorenyl moiety. This preference of the *gauche* conformation is consistent with the predictions from our dipole moment measurements, X-ray crystal diffraction measurements and AM1 calculations.

Table 4 lists the activation parameters of some 9,9'-disubstituted-9,9'-bifluorenyls (X = H, CH₃, Cl, Br, CN and NO₂). Comparison of the data clearly shows that the free energies of activation, defined as the difference in energy between the ground and transition states, vary in a manner which appears not to be correlated simply with a single parameter such as the steric interaction but is instead influenced also by other factors, e.g. the electronic properties of the substituents and the conjugative effects between the substituents and the fluorenyl moieties. In **1** and **2**, the *gauche* interactions between the adjacent polar substituents help to stabilize the ground state of the molecule.^{1,2} However, in the transition state for rotation there is less interaction between the substituents, so the energy of the transition state will be less affected by the nature of X. Thus a polar X such as CN and NO₂ will widen the energy difference between the ground state and transition state by decreasing the energy of the ground state and thus increasing the activation energy for exchange. AM1 calculations of the activation energies gave results which are much lower than the experimental values [16.38 and 26.59 kJ mol⁻¹ for **1** and **2**, respectively]. This discrepancy may be attributed to the underestimation of the rotational barrier around single bonds in AM1.³⁵

References

- R. J. W. LeFevre, G. L. D. Ritchie and P. J. Stiles, *J. Chem. Soc. B*, 1967, 819.
- Y. L. Lam, L. L. Koh and H. H. Huang, *J. Chem. Soc., Perkin Trans. 2*, 1993, 175.
- B. G. Tan, Y. L. Lam, H. H. Huang and L. H. L. Chia, *J. Chem. Soc., Perkin Trans. 2*, 1990, 2031.
- L. L. Koh, Y. L. Lam, K. Y. Sim and H. H. Huang, *Acta Crystallogr., Sect. B*, 1993, **49**, 116.
- Y. L. Lam, L. L. Koh and H. H. Huang, *J. Chem. Res. (M)*, 1991, 2119; *J. Chem. Res. (S)*, 1991, 212.
- L. H. L. Chia, H. H. Huang and P. K. K. Lim, *J. Chem. Soc. B*, 1969, 608.
- B. G. Tan, L. H. L. Chia, H. H. Huang, M. H. Kuok and S. H. Tang, *J. Chem. Soc., Perkin Trans. 2*, 1984, 1407.
- W. S. Matthews, J. E. Bares, J. E. Bartmess, F. G. Bordwell, F. J. Cornforth, G. E. Drucker, Z. Margolin, R. J. McCallum, G. J. McCollum and N. R. Vanier, *J. Am. Chem. Soc.*, 1975, **97**, 7006.
- W. Wislicenus and K. Russ, *Ber. Dtsch. Chem. Ges.*, 1910, **43**, 2719.
- M. S. Kharasch and G. Sosnovsky, *Tetrahedron*, 1958, **3**, 105.
- J. M. Birnie and N. Campbell, *Proc. R. Soc. Edinburgh, Sect. A*, 1969, **68**, 120.
- W. Wislicenus and M. Waldmüller, *Chem. Ber.*, 1908, **41**, 3338.
- A. H. Pagano and H. Shechter, *J. Org. Chem.*, 1970, **35**, 295.
- H. H. Huang and E. P. A. Sullivan, *Aust. J. Chem.*, 1968, **21**, 1721.
- R. J. W. LeFevre, *Dipole Moments*, 3rd edn., Methuen, London, 1953, ch. 2; *Adv. Phys. Org. Chem.*, 1965, **3**, 1.
- K. E. Calderbank, R. J. W. LeFevre and G. L. D. Ritchie, *J. Chem. Soc. B*, 1968, 503.
- M. J. S. Dewar, J. J. P. Stewart, J. M. Ruiz, D. Liotard, E. F. Kealy and R. D. Dennington II, AMPAC 5.0, Semichem Inc., USA, 1994.
- M. J. S. Dewar, E. G. Zoebisch, E. F. Healey and J. J. P. Stewart, *J. Am. Chem. Soc.*, 1985, **107**, 3902.
- W. Klyne and V. Prelog, *Experientia*, 1960, **16**, 521.
- Siemens, SHELXTL-PLUS, Release 4.20, Siemens Analytical X-ray Instruments Inc, Madison, Wisconsin, USA, 1990.
- R. J. W. LeFevre and H. Vine, *J. Chem. Soc.*, 1937, 1805.
- R. J. W. LeFevre and B. Orr, *Aust. J. Chem.*, 1964, **17**, 1098.
- K. K. Chui, H. H. Huang and P. K. K. Lim, *J. Chem. Soc.*, 1970, 304.
- D. A. Dougherty, K. Mislow, J. F. Blount, J. B. Wooten and J. Jacobus, *J. Am. Chem. Soc.*, 1977, **99**, 6149.
- J. Placek and F. Szöcs, *Macromol. Chem. Phys.*, 1994, **195**, 463.
- W. J. LeNoble, *Highlights of Organic Chemistry*, Marcel Dekker, New York, 1974, p. 626.
- D. A. Dougherty, F. M. Llort and K. Mislow, *Tetrahedron*, 1978, **34**, 1301.
- X. Solans and C. Miravittles, *Acta Crystallogr., Sect. B*, 1980, **36**, 2677.
- D. M. Burns and J. Iball, *Proc. R. Soc. London, A*, 1955, **227**, 200.
- K. S. Yong, Y. L. Lam, L. L. Koh, H. H. Huang and S. Y. Lee, *J. Mol. Struct.*, 1998, **442**, 145.
- L. L. Koh, H. H. Huang and K. Y. Sim, *Acta Crystallogr., Sect. C*, 1992, **48**, 1641.
- J. E. Lennard-Jones and H. H. M. Pike, *Trans. Faraday Soc.*, 1934, **30**, 830.
- Y. L. Lam, H. H. Huang and T. W. Hambley, *J. Chem. Soc., Perkin Trans. 2*, 1990, 2039.
- G. A. Olah, L. D. Field, M. I. Watkins and R. Malhotra, *J. Org. Chem.*, 1981, **46**, 1761.
- W. M. F. Fabian, *J. Comput. Chem.*, 1988, **9**, 369.

Paper 9/00968J